

Cost of Locally Approximating High-Dimensional Ground States of Contextual Quantum Models

Kaiyan Yang,^{1,*} Yanzheng Zhu,^{1,*} Xiao Zeng,¹ Zuoheng Zou,² Man-Hong Yung,² and Zizhu Wang^{1,†}

¹*Institute of Fundamental and Frontier Sciences and Ministry of Education Key Laboratory of Quantum Physics and Photonic Quantum Information, University of Electronic Science and Technology of China, Chengdu 611731, China*

²*Central Research Institute, Huawei Technologies, Shenzhen 518129, China*

Contextuality, one of the strongest forms of quantum correlations, delineates the quantum world and the classical one. It has been shown recently that some quantum models, in the form of infinite one-dimensional translation-invariant Hamiltonians with nearest- and next-to-nearest-neighbor interactions, have the lowest ground state energy density allowed in quantum physics. However, these models all have local Hilbert space dimension larger than two, making the study of their ground state behavior difficult on current qubit-based variational quantum simulation platforms. In this work, we focus on the cost of simulating the local approximations of ground states of these models using qubit-based parameterized quantum circuits. The local approximations, which are 3-site reduced density matrices with local Hilbert space dimension three, are purified then encoded into permutation-symmetric qubits. We develop a universal set of permutation-symmetry preserving qubit-based gates, using them as an ansatz to simulate parameterized quantum circuits designed for qutrits. These techniques allow us to assess the accuracy of simulating the purified local ground states with respect to a fixed amount of classical and quantum resources. We found that given the same quantum circuit and the number of iterations, more contextual ground states with lower energy density are easier to simulate.

CONTENTS

I. Introduction	1
II. Quantum Hamiltonians and local approximation of their ground states	2
III. Simulating qutrits on qubit-based parameterized quantum circuits	3
IV. Cost of locally approximating ground states of contextual Hamiltonians	5
V. Conclusions	10
References	10

I. INTRODUCTION

Exploring non-classical correlations present in many-body quantum systems has been an impetus for quantum simulation since its inception. While entanglement has always been the primary focus of this endeavor, the study of a stronger form of quantum correlation—contextuality—has recently been gaining popularity. Contextuality, both the Kochen-Specker type (Budroni *et al.*, 2022) and the Bell type (Brunner *et al.*, 2014; Cabello, 2021), has been shown

to be the source of quantum advantages in specific tasks in quantum computing (Bravyi *et al.*, 2018; Howard *et al.*, 2014) and quantum machine learning (Anshuetz *et al.*, 2023).

In an earlier work by some of the authors (Yang *et al.*, 2022), we found several infinite one-dimensional translation-invariant (TI) quantum Hamiltonians with nearest- and next-to-nearest-neighbor interactions have the lowest ground state energy density permissible in quantum physics. This lower bound is numerically certified by a variant of the NPA-hierarchy (Navascués *et al.*, 2007, 2008), and the quantum Hamiltonian achieving the bound has been found by optimizing the local observables of contextuality witnesses derived from Bell inequalities and computing their the ground state with uniform matrix product state (uMPS) algorithms (Cirac *et al.*, 2021; Haegeman *et al.*, 2011; Vanderstraeten *et al.*, 2019; Zauner-Stauber *et al.*, 2018). These quantum Hamiltonians, which are essentially many-body quantum Bell inequalities (Cirel'son, 1980), demarcate quantum and post-quantum theories, providing a conceptual way of experimentally refuting the universal validity of quantum physics (Yang *et al.*, 2022). In addition, they can be used in self-testing protocols (Šupić and Bowles, 2020) for many-body quantum systems, which has recently been done for entangled states in a network scenario (Šupić *et al.*, 2023). Self-testing can be seen as a method to separate classical control from quantum behavior (Reichardt *et al.*, 2013), leading to the central question of this work: How hard is it to generate local approxima-

* These authors contributed equally to this work

† zizhu@uestc.edu.cn

tions of ground states of quantum Hamiltonians that reach the lower bound?

In order to answer this question, we use variational quantum algorithms (VQAs) (Cerezo *et al.*, 2021) to simulate the purification of local reduced density matrices of ground states of quantum Hamiltonians exhibiting various degrees of contextuality. However, since these Hamiltonians all have local Hilbert space dimension 3 but our variational simulator is based on qubits, we encode a qutrit state into a pair of permutation-symmetric qubits. Exploiting permutation symmetry in many-body quantum systems allows us to characterize various forms of quantum correlations in many scenarios (Aulbach *et al.*, 2010; Markham, 2011; Ribeiro and Mosseri, 2011; Ribeiro *et al.*, 2008; Tura *et al.*, 2014, 2015; Wang and Markham, 2012). We also develop a qubit-based ansatz inspired by recent ansätze based on tensor network states (Ran, 2020; Rudolph *et al.*, 2023). Compared to earlier works using qubit-based variational algorithms to simulate higher-dimensional quantum systems (Gard *et al.*, 2020; Han *et al.*, 2024; Lyu *et al.*, 2023; Meyer *et al.*, 2023; Sawaya *et al.*, 2020), our ansatz preserves the permutation symmetry of the encoded states and allows arbitrary 2-qutrit gates to be implemented.

Using these techniques, we investigate the cost of locally simulating qutrit ground states of contextual quantum Hamiltonians from (Yang *et al.*, 2022) via qubit-based parameterized quantum circuits (PQCs). The cost is defined by comparing the negative logarithmic fidelity per site (NLF-per-site) of the PQC-generated state and the purified local ground state, with a fixed number of layers for the quantum circuit, thus fixing both the number of classical variational parameters and quantum gates. In addition, we also fix the number of iterations run by the classical optimization part of the VQA. A lower NLF-per-site signifies the two states are closer, making the simulation better. We observe that the cost to prepare the ground states that can exhibit contextuality are more expensive than the ground states that cannot. When the amount of violation becomes larger, the cost is gradually reduced while it still costs more resources than generating the states that cannot exhibit contextuality. When comparing these results to Hamiltonians which do not exhibit contextuality (often having separable ground states), the ground state energy density serves as a reliable indicator of the cost of approximating the local ground states of these classes of Hamiltonians with various degrees of contextuality witness violation.

II. QUANTUM HAMILTONIANS AND LOCAL APPROXIMATION OF THEIR GROUND STATES

In this work, the Hamiltonians we use are infinite one-dimensional translation-invariant with nearest- and next-to-nearest neighbor interactions, with each party having a choice of one of two dichotomic observables O_x, O_y with outcomes ± 1 . This class of Hamiltonians is called the 322-

type in (Yang *et al.*, 2022). They come from classical TI probability distributions, which form a convex polytope whose facets are contextuality witnesses:

$$\begin{aligned} & J_x \langle O_x^1 \rangle + J_y \langle O_y^1 \rangle + J_{xx}^{AB} \langle O_x^1 O_x^2 \rangle + J_{xy}^{AB} \langle O_x^1 O_y^2 \rangle \\ & + J_{yx}^{AB} \langle O_y^1 O_x^2 \rangle + J_{yy}^{AB} \langle O_y^1 O_y^2 \rangle + J_{xx}^{AC} \langle O_x^1 O_x^3 \rangle \\ & + J_{xy}^{AC} \langle O_x^1 O_y^3 \rangle + J_{yx}^{AC} \langle O_y^1 O_x^3 \rangle + J_{yy}^{AC} \langle O_y^1 O_y^3 \rangle \geq \mathcal{L}. \end{aligned} \quad (1)$$

where $\mathcal{J} \equiv \{J_x, J_y, J_{xx}^{AB}, J_{xy}^{AB}, J_{yx}^{AB}, J_{yy}^{AB}, J_{xx}^{AC}, J_{xy}^{AC}, J_{yx}^{AC}, J_{yy}^{AC}\}$ are coefficients of the contextuality witness, and \mathcal{L} is the classical bound. Quantum Hamiltonians are constructed from these witnesses by replacing O_x, O_y with local observables Σ_x, Σ_y :

$$\begin{aligned} H = & \sum_{i=1}^{\infty} J_x \Sigma_x^i + J_y \Sigma_y^i + J_{xx}^{AB} \Sigma_x^i \Sigma_y^{i+1} + J_{xy}^{AB} \Sigma_x^i \Sigma_y^{i+1} \\ & + J_{yx}^{AB} \Sigma_y^i \Sigma_x^{i+1} + J_{yy}^{AB} \Sigma_y^i \Sigma_y^{i+1} + J_{xx}^{AC} \Sigma_x^i \Sigma_x^{i+2} \\ & + J_{xy}^{AC} \Sigma_x^i \Sigma_y^{i+2} + J_{yx}^{AC} \Sigma_y^i \Sigma_x^{i+2} + J_{yy}^{AC} \Sigma_y^i \Sigma_y^{i+2}. \end{aligned} \quad (2)$$

After choosing suitable observables Σ_x and Σ_y , if the ground state energy density of (2) is smaller than \mathcal{L} , the quantum system is contextual. It is shown that in some 322-type Hamiltonians, to reach the lower limit of the ground state energy density, the local Hilbert space dimension must be at least 3 (see Table. I).

The ground state of Hamiltonian (2) is represented by a uMPS. A uMPS $|\phi(A)\rangle$ with the bond dimension D and the physical dimension d defined on an infinite 1D TI chain is parameterized by a set of $D \times D$ matrices $A^s (s = 1, 2, \dots, d)$. The overall TI variational ground state then can be written as

$$|\phi(A)\rangle = \sum_{\mathbf{s}} (\dots A^{s_{i-1}} A^{s_i} A^{s_{i+1}} \dots) |\mathbf{s}\rangle, \quad (3)$$

and represented diagrammatically as

$$|\phi(A)\rangle = \dots \text{---} \begin{array}{c} \text{---} \text{---} \text{---} \text{---} \text{---} \text{---} \\ | \quad | \quad | \quad | \quad | \\ \text{---} \text{---} \text{---} \text{---} \text{---} \end{array} \text{---} \dots$$

Since the ground state is defined on an infinite chain, we can only simulate its local approximation. The 3-site local reduced state of the ground state $|\phi(A)\rangle$ is

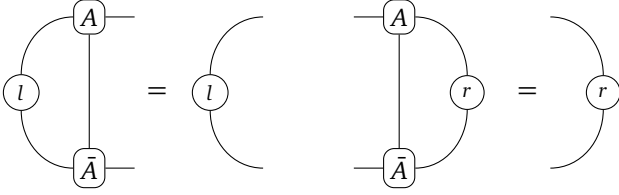
$$\rho_3 = \begin{array}{c} \text{---} \text{---} \text{---} \text{---} \text{---} \text{---} \\ | \quad | \quad | \quad | \quad | \\ \text{---} \text{---} \text{---} \text{---} \text{---} \end{array} \quad (4)$$

Here, l and r are the left and right fixed points of the transfer matrix $T = \sum_s \bar{A}^s \otimes A^s$ with non-degenerate leading

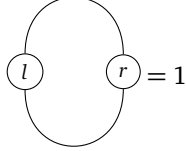
TABLE I Five many-body contextuality witnesses can be maximally violated by the ground states of 1D infinite TI Hamiltonians, where \mathcal{L} is classical bound, $\mathcal{J} \equiv \{J_x, J_y, J_{xx}^{AB}, J_{xy}^{AB}, J_{yx}^{AB}, J_{yy}^{AB}, J_{xx}^{AC}, J_{xy}^{AC}, J_{yx}^{AC}, J_{yy}^{AC}\}$ is the coefficients of contextuality witness which is also couplings of the Hamiltonian (2), and Q_{Limit} is the maximal quantum violation obtained when the local physical dimension is 3.

No.	\mathcal{L}	J_x	J_y	J_{xx}^{AB}	J_{xy}^{AB}	J_{yx}^{AB}	J_{yy}^{AB}	J_{xx}^{AC}	J_{xy}^{AC}	J_{yx}^{AC}	J_{yy}^{AC}	Q_{Limit}
1	-6	-6	0	2	3	3	-2	3	-1	-1	1	-6.32747
2	-6	-4	2	2	2	2	-4	1	-1	-1	3	-6.33712
3	-3	-3	1	1	1	1	-1	1	0	-1	1	-3.20711
4	-4	-2	-2	-2	1	-1	-2	1	0	2	1	-4.14623
5	-8	-11	1	5	2	2	-1	4	-1	-2	1	-8.12123

eigenvalue 1. Diagrammatically, l and r satisfy



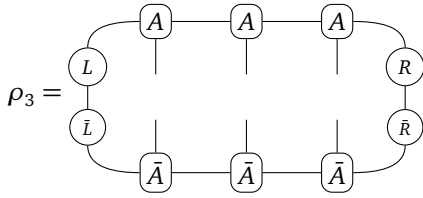
Besides, l and r satisfy the normalization condition $\text{Tr}(lr) = 1$, or, diagrammatically,



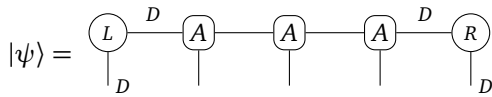
Unless $D = 1$, ρ_3 is a mixed state. To prepare ρ_3 via quantum circuits, we need to purify ρ_3 to a pure state $|\psi\rangle$. First, we perform Cholesky decomposition on l and r :

$$l = L^\dagger L, \quad r = RR^\dagger.$$

ρ_3 is then represented by

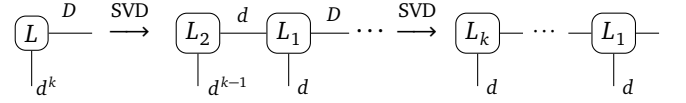


Then, we split ρ_3 into top and bottom parts. The top part is the target state $|\psi\rangle$



However, the physical dimension of L and R is not d , so we express L and R using $k = \lceil \log_d D \rceil$ tensors with physical dimension d (assuming $D > d$). If $\log_d D = k$ is an integer,

we repeatedly apply singular value decompositions (SVDs) to L and R



Similarly, we repeatedly do SVDs on R and get tensors $\{R_1, \dots, R_k\}$. Replacing L and R with $\{L_1, \dots, L_k\}$ and $\{R_1, \dots, R_k\}$ respectively, we finally get the purified state. If $\log_d D$ is not an integer, we enlarge the physical dimension of L to d^k by adding zeros to L , and then repeatedly do SVDs as before.

III. SIMULATING QUTRITS ON QUBIT-BASED PARAMETERIZED QUANTUM CIRCUITS

Even though the purification procedure above works for any local Hilbert space dimension, the Hamiltonians maximally violating the five witnesses in Table. I all have local dimension 3, which will be our focus for the rest of this work. After obtaining the purified qutrit MPS via the purification procedure, we need to variationally prepare them using QOCs. A good ansatz allows the simulation to be done efficiently and accurately. The ansatz we use consists of stacked linear layers of two-qutrit parameterized unitaries, similar to the one used for qubits in Ref. (Ran, 2020; Rudolph et al., 2023). We purify the 3-site local reduced state to a 7-site pure state $|\psi(A, L_1, L_2, R_1, R_2)\rangle$, and the quantum circuit with two layers is given by Fig. 1, where $\{\theta_k\}$ is a set of parameters and $\{U(\theta_k)\}$ is a set of parameterized two-qutrit unitaries. The ansatz above can approximate $|\psi\rangle$ up to very high accuracy, with proper optimization techniques (Rudolph et al., 2023). It is also a typical case of the finite local-depth circuit (FLDC) described in (Zhang et al., 2024), which is shown to be free from the barren plateaux problem.

However, $\{U(\theta_k)\}$ in Fig. 1 are qutrit unitaries. In order to simulate the purified local ground states on qubit-based platforms, we encode each qutrit into a pair of permutation-symmetric qubits and develop a universal set of permutation-symmetry preserving qubits gates to approximate any 2-qutrit gate. Existing encoding methods

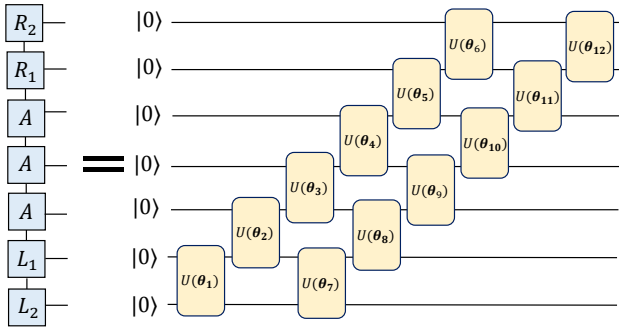


FIG. 1 Example of quantum circuit with two layers for 7-site MPS $|\psi(A, L_1, L_2, R_1, R_2)\rangle$.

which allow the simulation of high-dimensional quantum systems on qubit-based VQAs typically use standard binary, Gray code, or unary encoding (Sawaya *et al.*, 2020). They do not guarantee that the encoded states stay in the encoded subspace through gate operations. Our gate operations preserve the symmetry of encoded qubits. Similar encoding methods based on symmetry has been applied to quantum chemistry simulation (Gard *et al.*, 2020), variational quantum spin eigensolver (Lyu *et al.*, 2023), variational quantum machine learning (Meyer *et al.*, 2023), and multilevel variational spectroscopy simulator (Han *et al.*, 2024). However, as noted below, our method differs from these one substantially.

The Hilbert space of a d -dimensional ($d \geq 3$) qudit is isomorphic to the symmetric subspace \mathcal{H}_s of the n -qubit system, where $n = d - 1$ and \mathcal{H}_s is spanned by the Dicke basis $\{|S_m\rangle : 0 \leq m \leq n\}$ (Dicke, 1954)

$$|S_m\rangle = \binom{n}{m}^{-1/2} \sum_{\text{perm}} |1\rangle^{\otimes m} |0\rangle^{\otimes (n-m)}. \quad (5)$$

$|S_m\rangle$ is the coherent superposition of all permutations of the computational basis states with m qubits being $|1\rangle$ and $n - m$ qubits being $|0\rangle$. The Hilbert space for two qubits \mathcal{H}_4 can be decomposed into the direct sum of the three-dimensional symmetric subspace \mathcal{H}_s and the one-dimensional anti-symmetric subspace \mathcal{H}_a spanned by the anti-symmetric basis $|S_a\rangle = (|01\rangle - |10\rangle)/\sqrt{2}$, i.e. $\mathcal{H}_4 = \mathcal{H}_s \oplus \mathcal{H}_a$.

Denote the qutrit Hilbert space by \mathcal{H}_3 with basis $\{|0\rangle, |1\rangle, |2\rangle\}$. For a qutrit state $|\psi\rangle = \psi_0|0\rangle + \psi_1|1\rangle + \psi_2|2\rangle$, we define the symmetric encoded state as $|\psi\rangle_{\text{enc}} = \psi_0|S_0\rangle + \psi_1|S_1\rangle + \psi_2|S_2\rangle$, where $|S_0\rangle = |00\rangle, |S_1\rangle = \frac{1}{\sqrt{2}}(|01\rangle + |10\rangle), |S_2\rangle = |11\rangle$.

Qubit gates may map a symmetric state $|\psi\rangle_{\text{enc}}$ out of \mathcal{H}_s . To make sure we always operate in \mathcal{H}_s thus do not increase the total Hilbert space dimension of the VQA, we need gates that are symmetry-preserving. Even though Ref. (Gard *et al.*, 2020; Lyu *et al.*, 2023) both incorporate symmetries into circuit design, the space they considered is the linear span of all permutations of the state $|1\rangle^{\otimes m} |0\rangle^{\otimes (n-m)}$ in the

Dicke state $|S_m\rangle$. Moreover, the circuits they used are designed to preserve different kinds of symmetries (like total spin), which helps to improve accuracy and reduce computational resources. Our circuit design contains a universal gate set for simulating any qutrit gates with qubit gates, and the gate set is symmetry-preserving.

Let $U \in U(3)$ be a qutrit gate. Then, U can be written as

$$U = \sum_{i,j=0}^2 u_{ij} |i\rangle \langle j|. \quad (6)$$

Applying the symmetric state encoding on the computational basis states $|i\rangle$ and $\langle j|$, $i, j \in \{0, 1, 2\}$, U can be encoded as \tilde{U} in terms of Dicke basis $\{|S_0\rangle, |S_1\rangle, |S_2\rangle\}$:

$$\tilde{U} = \sum_{i,j=0}^2 u_{ij} |S_i\rangle \langle S_j|. \quad (7)$$

However, \tilde{U} is not a unitary in $U(4)$ because the anti-symmetric component is missing. By adding a projector $P = |S_a\rangle \langle S_a|$, where $|S_a\rangle = (|01\rangle - |10\rangle)/\sqrt{2}$ is the anti-symmetric basis of \mathcal{H}_4 , U can be encoded as a two-qubit unitary U_{enc} :

$$U_{\text{enc}} = \tilde{U} + P. \quad (8)$$

The fact that U_{enc} is a unitary can be seen from

$$\begin{aligned} U_{\text{enc}} U_{\text{enc}}^\dagger &= (\tilde{U} + P)(\tilde{U} + P)^\dagger \\ &= \left(\sum_{i,k=0}^2 u_{ik} |S_i\rangle \langle S_k| + P \right) \left(\sum_{t,j=0}^2 u_{tj} |S_t\rangle \langle S_j| + P \right)^\dagger \\ &= \sum_{i,j=0}^2 \left(\sum_{k=0}^2 u_{ik} u_{kj}^* \right) |S_i\rangle \langle S_j| + |S_a\rangle \langle S_a| \\ &= \sum_{i,j=0}^2 \delta_{ij} |S_i\rangle \langle S_j| + |S_a\rangle \langle S_a| \\ &= \sum_{i=0}^2 |S_i\rangle \langle S_i| + |S_a\rangle \langle S_a| = \mathbb{I}_4 \end{aligned} \quad (9)$$

U_{enc} is also symmetry-preserving, since U operating on $|\psi\rangle$ is equivalent to U_{enc} operating on $|\psi\rangle_{\text{enc}}$:

$$\begin{aligned} U_{\text{enc}} |\psi\rangle_{\text{enc}} &= (\tilde{U} + P) |\psi\rangle_{\text{enc}} \\ &= \left(\sum_{i,j=0}^2 u_{ij} |S_i\rangle \langle S_j| + |S_a\rangle \langle S_a| \right) \left(\sum_{k=0}^2 \psi_k |S_k\rangle \right) \\ &= \sum_{i,j=0}^2 u_{ij} \psi_j |S_i\rangle = (U |\psi\rangle)_{\text{enc}} \end{aligned} \quad (10)$$

Universal gate sets for higher-dimensional gates have been studied since the 1990s (Gottesman, 1999; Luo and Wang, 2014; Muthukrishnan and Stroud Jr, 2000).

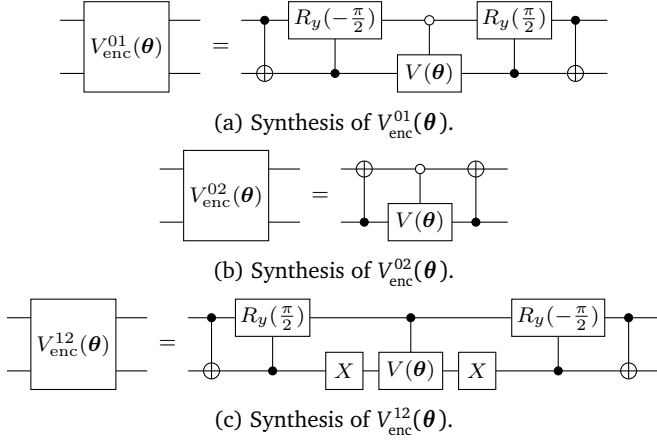


FIG. 2 The circuit for synthesizing two-qubit symmetry-preserving unitaries $V_{\text{enc}}^{01}(\theta)$ in (a), $V_{\text{enc}}^{02}(\theta)$ in (b) and $V_{\text{enc}}^{12}(\theta)$ in (c). ● denotes the control state is $|1\rangle$, and ○ denotes the control state is $|0\rangle$. R_y represents the rotation-y gate, X denotes Pauli X gate, and $V(\theta) \in U(2)$ has the general form of (13).

Ref. (Di and Wei, 2013, 2015) provide an optimal method for synthesizing qutrit unitaries with a universal gate set using quantum Shannon decomposition (Shende *et al.*, 2006). Using this gate encoding method, we encode each qutrit gate in the universal qutrit gate set into symmetry-preserving qubit gates. Then, we propose a universal qubit gate set to approximate those symmetry-preserving qubit gates.

Given an arbitrary single-qutrit unitary $U \in U(3)$, using Gaussian elimination, it can be decomposed as

$$U = V^{01}V^{02}V^{12}, \quad (11)$$

where $V^{ij} \in U(3)$, $(i, j) \in \{(0, 1), (0, 2), (1, 2)\}$ are two-level qutrit unitary gates with the general form

$$V^{01} = \begin{bmatrix} \theta_1 & \theta_2 & 0 \\ \theta_3 & \theta_4 & 0 \\ 0 & 0 & 1 \end{bmatrix}, \quad V^{02} = \begin{bmatrix} \theta_1 & 0 & \theta_2 \\ 0 & 1 & 0 \\ \theta_3 & 0 & \theta_4 \end{bmatrix}, \quad V^{12} = \begin{bmatrix} 1 & 0 & 0 \\ 0 & \theta_1 & \theta_2 \\ 0 & \theta_3 & \theta_4 \end{bmatrix}. \quad (12)$$

Here, $\theta_1, \theta_2, \theta_3$ and θ_4 are the entries of an qubit unitary $V(\theta) \in U(2)$:

$$V(\theta) = \begin{bmatrix} \theta_1 & \theta_2 \\ \theta_3 & \theta_4 \end{bmatrix}, \quad (13)$$

By implementing the gate encoding method on $V^{ij}(\theta)$, we obtain the two-qubit symmetry-preserving unitary $V_{\text{enc}}^{ij}(\theta)$. The circuit for synthesizing $V_{\text{enc}}^{01}(\theta)$, $V_{\text{enc}}^{02}(\theta)$ and $V_{\text{enc}}^{12}(\theta)$ are shown in Fig. 2.

We need to encode two-qutrit unitaries into qubit gates as required by our ansatz. The Ref. (Di and Wei, 2015) provides a method consisting of single-qutrit gates, controlled diagonal gates and uniformly controlled R_y rotation gates to synthesize a generic N -qutrit ($N \geq 2$) circuit. Combined with the method for synthesizing the controlled diagonal

gates proposed in (Di and Wei, 2013), an arbitrary two-qutrit unitary gate $U \in U(9)$ can be synthesized as shown in Fig. 3.

The circuit in Fig. 3 includes only two types of qutrit gates: (i) single-qutrit gates and (ii) qutrit two-level controlled rotation gates, both of which can be encoded by our gate encoding method. All encoded single-qutrit gates can be decomposed into two-qubit gates using the decomposition in (11) and synthesis method in Fig. 2. For the encoded qutrit two-level controlled rotation gates, according to the specific state of the control, they can be decomposed into qubit-based gates in Fig. 4. Note that the two-qubit gate V_{enc}^{ij} in Fig. 4 is the two-qubit gate in Fig. 2 for $(i, j) \in \{(0, 1), (0, 2), (1, 2)\}$.

From the state encoding method, we know that the n -qutrit Hilbert space is isomorphic to the symmetric subspace of the $2n$ -qubit space. From the gate encoding method, we know the encoded qutrit gate is symmetry-preserving. From these plus the universality of qutrit gates proposed in (Di and Wei, 2015), we conclude that the qubit-based gates in Fig. 2 and in Fig. 3 form a universal gate set that can approximate arbitrary symmetry-preserving qubit-gates.

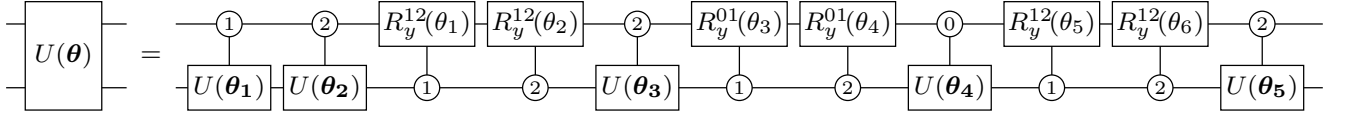
IV. COST OF LOCALLY APPROXIMATING GROUND STATES OF CONTEXTUAL HAMILTONIANS

We apply the state and gate encoding methods presented above to our qubit-based PQC to locally simulate qutrit ground states of five types of Hamiltonians in (2). The Hamiltonians have different sets of couplings \mathcal{J} given by five contextuality witnesses shown in Table. I. Given each contextuality witness, the set of couplings \mathcal{J} in Hamiltonian (2) is determined and each of qutrit local observables $\{\Sigma_a : a \in \{x, y\}\}$ being a real projective measurement is parameterized as

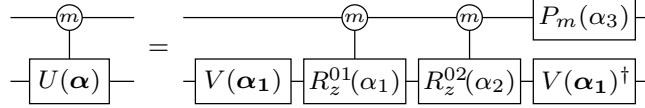
$$\Sigma_a(w_a) = (e^{\sum_{k=1}^3 w_{ak} S_k}) \Lambda_a (e^{\sum_{k=1}^3 w_{ak} S_k})^T, \quad (14)$$

where Λ_a is a diagonal matrix with entries ± 1 , $\{S_k\}$ are the basis of three-dimensional skew-symmetric matrices space, and $w_a \equiv (w_{a1}, w_{a2}, w_{a3})$ are real parameters. Here, all parameters are denoted as $W \equiv (w_x, w_y)$. Then, given a set of parameters W , the Hamiltonian is specified and the ground state can be computed using MPS-based algorithms such as the time-dependent variational principle (TDVP) algorithm (Haegeman *et al.*, 2011) or the variational uniform matrix product state (VUMPS) algorithm (Vanderstraeten *et al.*, 2019; Zauner-Stauber *et al.*, 2018).

Beginning with a set of random parameters W , the local observables are optimized using gradient descent aiming at finding the lowest possible ground state energy density. We follow the trajectory of the gradient descent and obtain a sequence of Hamiltonians having the same \mathcal{J} but different local observables. From these, we obtain a sequence of qutrit MPS ground states of contextual Hamiltonian exhibiting different amounts of quantum violations. In Fig. 5,

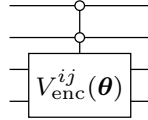


(a) Synthesis of an arbitrary two-qutrit unitary $U \in U(9)$ consisting of qutrit-controlled unitary gates and qutrit two-level controlled rotation gates. \circ denotes the control, with the number (0, 1 or 2) inside representing the state it is in. Note that each qutrit-controlled unitary gate can be further decomposed into single-qutrit gates and qutrit two-level controlled rotation gates, with the decomposition shown in (b).

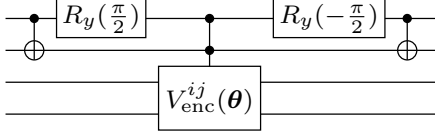


(b) Synthesis of qutrit controlled unitary gates in (a). \circ denotes the control in state $|m\rangle$ with $m = 0, 1, 2$. R_z^{01} and R_z^{02} are qutrit two-level rotation gates, P_m is the qutrit phase gate with respect to the control state $|m\rangle$, and $V \in U(3)$ is a single-qutrit gate constrained by the diagonal decomposition $U = VDV^\dagger$ for a diagonal matrix D .

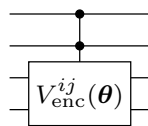
FIG. 3 The circuit for synthesizing an arbitrary two-qutrit unitary $U \in U(9)$. (a) Synthesis of U in terms of qutrit controlled unitary gates and qutrit two-level controlled rotation gates. (b) Synthesis of qutrit controlled unitary gates in (a) in terms of single-qutrit gates and qutrit two-level controlled rotation gates. Combining (a) and (b), the circuit for synthesizing two-qutrit unitary U consists only single-qutrit gates and qutrit two-level controlled rotation gates.



(a) Circuit of encoded qutrit two-level controlled rotation gates when the control state is $|0\rangle$ in Fig. 3.



(b) Circuit of encoded qutrit two-level controlled rotation gates when the control state is $|1\rangle$ in Fig. 3. Here, R_y is the single-qubit rotation gate.



(c) Circuit of encoded qutrit two-level controlled rotation gates when the control state is $|2\rangle$ in Fig. 3.

FIG. 4 The circuit for the encoded qutrit two-level controlled rotation gates in Fig. 3. According to the specific state of the control, they can be decomposed into three cases. (a) Circuit for encoded qutrit two-level controlled rotation gates when the control state is $|0\rangle$. (b) Circuit for encoded qutrit two-level controlled rotation gates when the control state is $|1\rangle$. (c) Circuit for encoded qutrit two-level controlled rotation gates when the control state is $|2\rangle$. In all subplots, the two-qubit gate V_{enc}^{ij} is the two-qubit gate in Fig. 2 for $(i, j) \in \{(0, 1), (0, 2), (1, 2)\}$.

each point represents a specific Hamiltonian on the trajectory and different colors represent different bond dimensions D of the uMPS ground states. For each model, five possibilities $D = 5, 6, 7, 8, 9$ and 3-site local approximations of ground states are considered. Using the purification proce-

dures in Sec. II, we obtain the purified ground states, which are 7-site qutrit MPSs $|\psi(A, L_1, L_2, R_1, R_2)\rangle$ with respect to $D \in \{5, 6, 7, 8, 9\}$. These qutrit states are then generated by the quantum circuit consisting of stacked two layers of two-qutrit unitaries in Fig. 1.

To simulate the purified qutrit states on qubit-based quantum circuits, we encode all these 7-site qutrit MPSs $|\psi(A, L_1, L_2, R_1, R_2)\rangle$ into the 14-site qubit states by the symmetric state encoding method, and the encoded qubit states are our target states $|\psi\rangle_T$. Besides, using the gate encoding method and the circuits for synthesizing symmetry-preserving gates, each qutrit gate $U(\theta)$ in the quantum circuit in Fig. 1 can be synthesized by the circuit consisting of qubit gates $U_{\text{enc}}(\theta)$ with trainable parameters θ in Fig. 6. Then, we use the same qubit-based PQC to simulate all the target 14-site qubit states. This means that all target states are approximated by the same quantum circuit. Each state $|\psi\rangle_{\text{QC}}$ generated by the quantum circuit is truncated after 500 iterations. Then, we calculate the negative logarithmic fidelity per site (NLF-per-site) \mathcal{F} between the target state $|\psi\rangle_T$ and $|\psi\rangle_{\text{QC}}$:

$$\mathcal{F} = -\frac{\ln \sqrt{\langle \psi_{\text{QC}} | \psi \rangle_T \langle \psi | \psi_{\text{QC}} \rangle}}{N}, \quad (15)$$

where N is the number of qubits for the target state. In this situation, if two target states $|\psi_1\rangle_T$ and $|\psi_2\rangle_T$ have the same bond dimension D , and $|\psi_1\rangle_{\text{QC}}$ has a lower NLF-per-site than $|\psi_2\rangle_{\text{QC}}$, then we conclude that preparing $|\psi_1\rangle_T$ consumes fewer circuit resources than preparing $|\psi_2\rangle_T$.

We carry out the simulation on the MindQuantum platform (MindQuantum Developer, 2021) and the results are shown in Fig. 5. Each sub-figure corresponds to one contextuality witness, and each point in the sub-figure corresponds to one ground state of the Hamiltonian with form (2) when

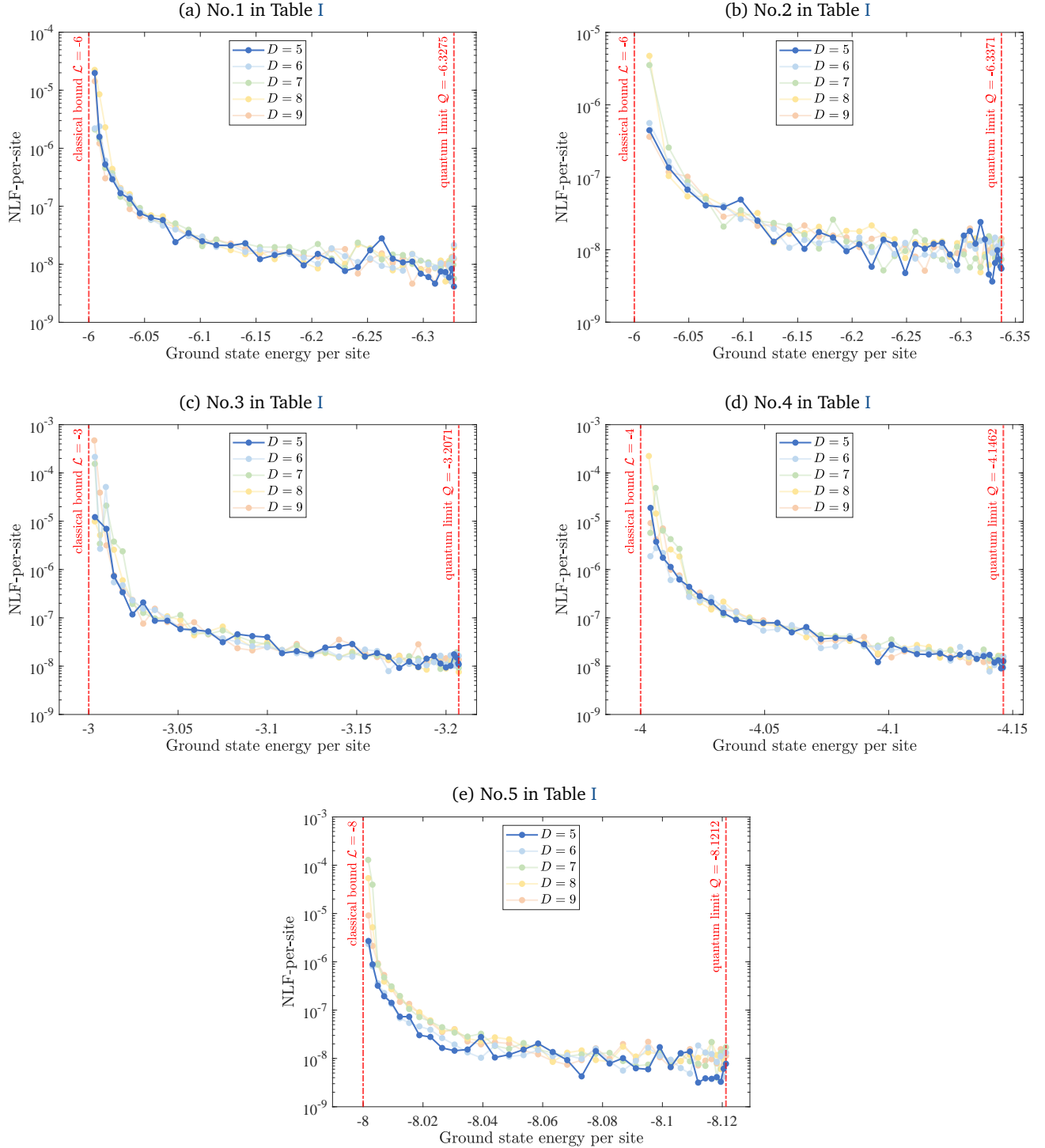
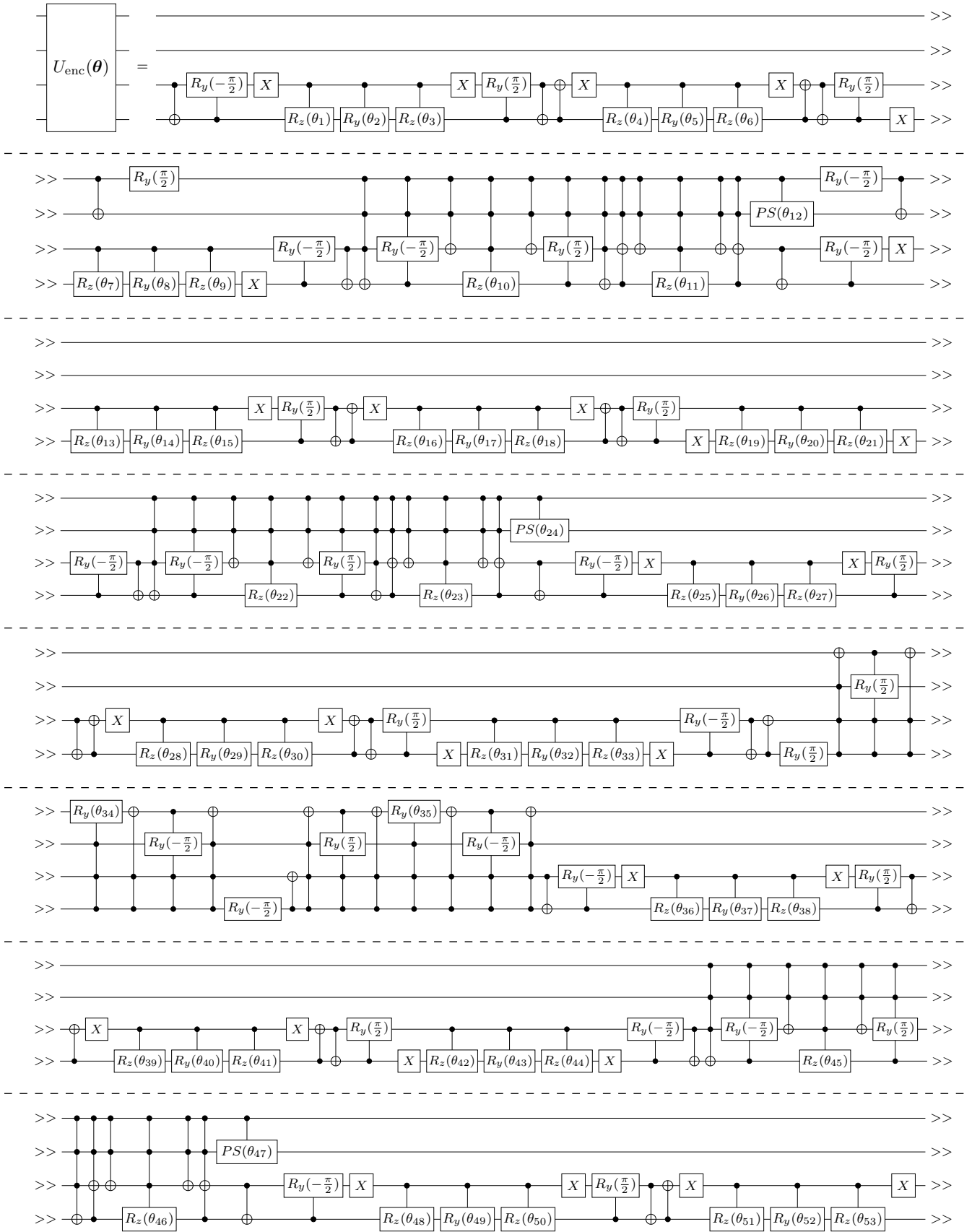


FIG. 5 The NFL-per-site of purified 3-site local approximation of ground states with bond dimensions $D = 5, 6, 7, 8, 9$ of five contextual witnesses in Table I versus a sequence of ground state energy densities when the local dimension $d = 3$. All the target states $|\psi\rangle_T$ are the 14-site qubit state. In each subplot, each point represents a specific Hamiltonian on the trajectory and different colors represent different bond dimensions D of the uMPS ground states.



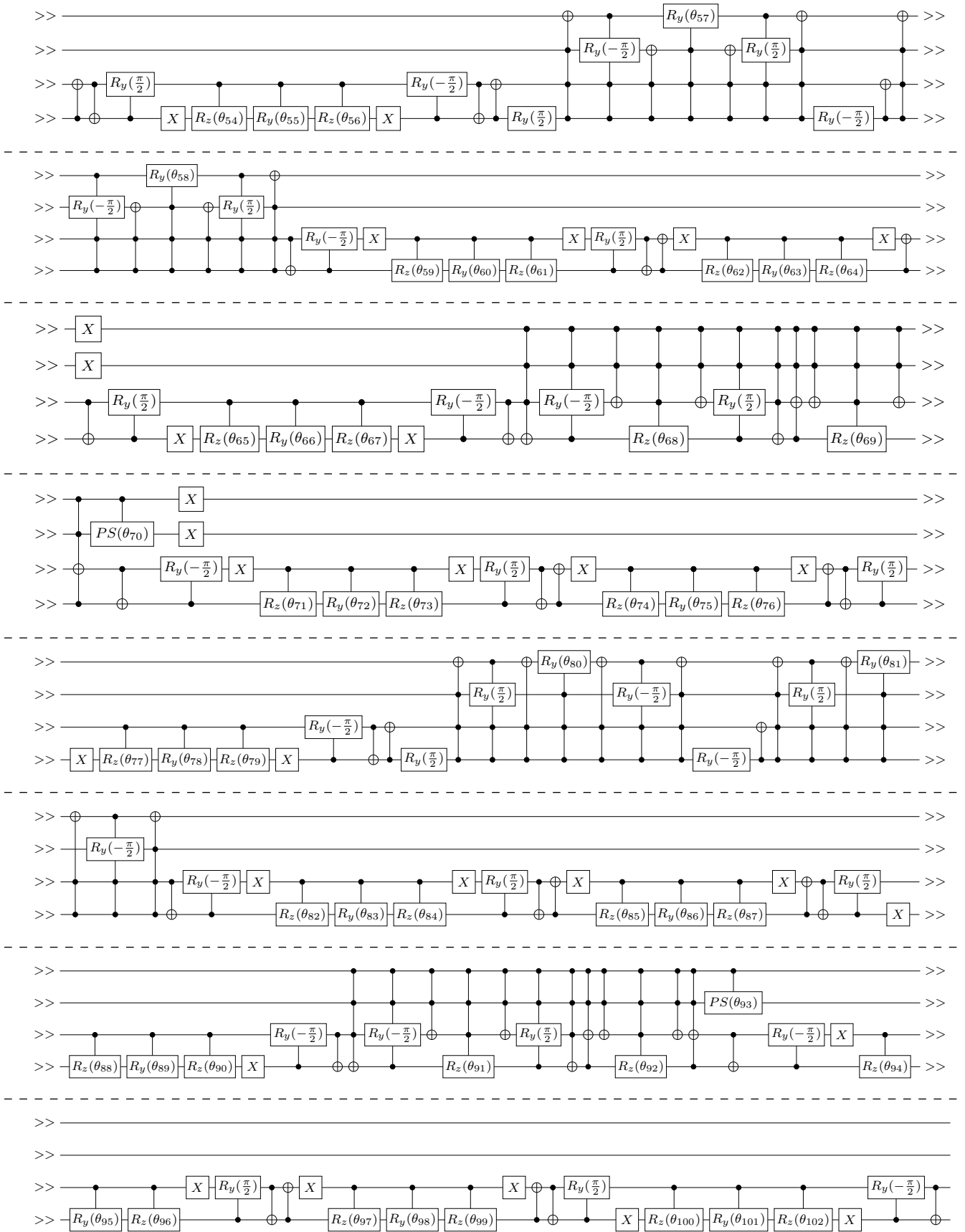


FIG. 6 Symmetry-preserving 4-qubit circuit for synthesising arbitrary two-qubit unitary gates $U(\theta)$ in Fig. 1.

the local physical dimension is 3. we find that the circuit resources to simulate the ground states that can exhibit contextuality are more expensive than the ground states that cannot. As shown in Table. II, using the same circuit resources as generating the contextual ground states, the NLF-per-site of each ground state with the ground state energy density being the classical bound is much smaller than the contextual ones. More interestingly, as the ground state energy density decreases, or equivalently, as the amount of violation to contextuality witness becomes larger, the NLF-per-site becomes smaller. This indicates that the stronger contextuality exhibited by the ground state, the less circuit resources are required to prepare the state.

TABLE II NLF-per-site for the ground state that can not exhibit contextuality and have the the ground state energy density being the classical bounds.

No.	\mathcal{L}	D	NLF-per-site
1	-6	1	3.700743415417188e-17
2	-6	1	1.110223024625156e-16
3	-3	1	2.590520390792030e-16
4	-4	1	2.220446049250312e-16
5	-8	3	4.344672769700346e-14

V. CONCLUSIONS

In this paper, we investigate the connection between contextuality and circuit resources required to simulate local approximation to the ground states of maximally contextual quantum Hamiltonians. Since maximal quantum violation demands qutrit systems, we propose a symmetric encoding framework that enables the simulation of any qutrit state using qubit-based parameterized quantum circuits. We found that generating ground states exhibiting contextuality consumes more circuit resources than those that do not exhibit contextuality. We find that, given the same amount of classical and quantum resources, the more contextual a Hamiltonian becomes, the easier it is to faithfully simulate its local ground state. High-dimensional quantum circuit platforms have wide applications in the fields of quantum computing and quantum simulation. Our proposed universal gate set plays a central role in this context. However, considering the synthesis of high-dimensional gates, there is room for improvement in the number of CNOTs, multi-controlled gates, and the corresponding circuit structure in the future.

REFERENCES

Anschuetz, Eric R, Hong-Ye Hu, Jin-Long Huang, and Xun Gao (2023), “Interpretable quantum advantage in neural sequence learning,” *PRX Quantum* **4**, 020338.

Aulbach, Martin, Damian Markham, and Mio Muraio (2010), “The maximally entangled symmetric state in terms of the geometric measure,” *New Journal of Physics* **12** (7), 073025.

Bravyi, Sergey, David Gosset, and Robert König (2018), “Quantum advantage with shallow circuits,” *Science* **362** (6412), 308–311.

Brunner, Nicolas, Daniel Cavalcanti, Stefano Pironio, Valerio Scarani, and Stephanie Wehner (2014), “Bell nonlocality,” *Rev. Mod. Phys.* **86**, 419–478.

Budroni, Costantino, Adán Cabello, Otfried Gühne, Matthias Kleinmann, and Jan-Åke Larsson (2022), “Kochen-specker contextuality,” *Rev. Mod. Phys.* **94**, 045007.

Cabello, Adán (2021), “Bell Non-locality and Kochen–Specker Contextuality: How are They Connected?” *Foundations of Physics* **51** (3), 61.

Cerezo, M, Andrew Arrasmith, Ryan Babbush, Simon C. Benjamin, Suguru Endo, Keisuke Fujii, Jarrod R. McClean, Kosuke Mitarai, Xiao Yuan, Lukasz Cincio, and Patrick J. Coles (2021), “Variational quantum algorithms,” *Nature Reviews Physics* **3** (9), 625–644.

Cirac, J Ignacio, David Pérez-García, Norbert Schuch, and Frank Verstraete (2021), “Matrix product states and projected entangled pair states: Concepts, symmetries, theorems,” *Rev. Mod. Phys.* **93**, 045003.

Cirel’son, Boris S (1980), “Quantum generalizations of Bell’s inequality,” *Letters in Mathematical Physics* **4**, 93–100.

Di, Yao-Min, and Hai-Rui Wei (2013), “Synthesis of multivalued quantum logic circuits by elementary gates,” *Physical Review A* **87** (1), 012325.

Di, Yao-Min, and Hai-Rui Wei (2015), “Optimal synthesis of multivalued quantum circuits,” *Physical Review A* **92** (6), 062317.

Dicke, Robert H (1954), “Coherence in spontaneous radiation processes,” *Physical Review* **93**, 99–110.

Gard, Bryan T, Linghua Zhu, George S Barron, Nicholas J Mayhall, Sophia E Economou, and Edwin Barnes (2020), “Efficient symmetry-preserving state preparation circuits for the variational quantum eigensolver algorithm,” *npj Quantum Information* **6** (1), 10.

Gottesman, Daniel (1999), “Fault-tolerant quantum computation with higher-dimensional systems,” in *Quantum Computing and Quantum Communications*, edited by Colin P. Williams, pp. 302–313.

Haegeman, Jutho, J. Ignacio Cirac, Tobias J. Osborne, Iztok Pižorn, Henri Verschelde, and Frank Verstraete (2011), “Time-dependent variational principle for quantum lattices,” *Physical Review Letters* **107**, 070601.

Han, Zhikun, Chufan Lyu, Yuxuan Zhou, Jiahao Yuan, Ji Chu, Wuerkaixi Nuerbolati, Hao Jia, Lifu Nie, Weiwei Wei, Zusheng Yang, Libo Zhang, Ziyang Zhang, Chang-Kang Hu, Ling Hu, Jian Li, Dian Tan, Abolfazl Bayat, Song Liu, Fei Yan, and Dapeng Yu (2024), “Multilevel variational spectroscopy using a programmable quantum simulator,” *Physical Review Research* **6**, 013015.

Howard, Mark, Joel Wallman, Victor Veitch, and Joseph Emerson (2014), “Contextuality supplies the ‘magic’ for quantum computation,” *Nature* **510** (7505), 351–355.

Luo, MingXing, and XiaoJun Wang (2014), “Universal quantum computation with qudits,” *Science China Physics, Mechanics & Astronomy* **57** (9), 1712–1717.

Lyu, Chufan, Xusheng Xu, Man-Hong Yung, and Abolfazl Bayat (2023), “Symmetry enhanced variational quantum spin eigensolver,” *Quantum* **7**, 899.

Markham, Damian (2011), “Entanglement and symmetry in permutation-symmetric states,” *Phys. Rev. A* **83** (4), 042332.

- Meyer, Johannes Jakob, Marian Mularski, Elies Gil-Fuster, Antonio Anna Mele, Francesco Arzani, Alissa Wilms, and Jens Eisert (2023), “Exploiting symmetry in variational quantum machine learning,” *PRX Quantum* **4**, 010328.
- MindQuantum Developer, (2021), “MindQuantum, version 0.6.0,” .
- Muthukrishnan, Ashok, and Carlos R Stroud Jr (2000), “Multivalued logic gates for quantum computation,” *Physical Review A* **62**, 052309.
- Navascués, Miguel, Stefano Pironio, and Antonio Acín (2007), “Bounding the set of quantum correlations,” *Physical Review Letters* **98**, 010401.
- Navascués, Miguel, Stefano Pironio, and Antonio Acín (2008), “A convergent hierarchy of semidefinite programs characterizing the set of quantum correlations,” *New Journal of Physics* **10** (7), 073013.
- Ran, Shi-Ju (2020), “Encoding of matrix product states into quantum circuits of one- and two-qubit gates,” *Physical Review A* **101**, 032310.
- Reichardt, Ben W, Falk Unger, and Umesh Vazirani (2013), “Classical command of quantum systems,” *Nature* **496** (7446), 456–460.
- Ribeiro, Pedro, and Rémy Mosseri (2011), “Entanglement in the Symmetric Sector of n Qubits,” *Phys. Rev. Lett.* **106** (18), 180502.
- Ribeiro, Pedro, Julien Vidal, and Rémy Mosseri (2008), “Exact spectrum of the Lipkin-Meshkov-Glick model in the thermodynamic limit and finite-size corrections,” *Phys. Rev. E* **78**, 021106.
- Rudolph, Manuel S, Jing Chen, Jacob Miller, Atithi Acharya, and Alejandro Perdomo-Ortiz (2023), “Decomposition of matrix product states into shallow quantum circuits,” *Quantum Science and Technology* **9** (1), 015012.
- Sawaya, Nicolas PD, Tim Menke, Thi Ha Kyaw, Sonika Johri, Alán Aspuru-Guzik, and Gian Giacomo Guerreschi (2020), “Resource-efficient digital quantum simulation of d-level systems for photonic, vibrational, and spin-s hamiltonians,” *npj Quantum Information* **6** (1), 49.
- Shende, Vivek V, Stephen S. Bullock, and Igor L. Markov (2006), “Synthesis of quantum-logic circuits,” *IEEE Transactions on Computer-Aided Design of Integrated Circuits and Systems* **25** (6), 1000–1010.
- Šupić, Ivan, and Joseph Bowles (2020), “Self-testing of quantum systems: a review,” *Quantum* **4**, 337.
- Šupić, Ivan, Joseph Bowles, Marc-Olivier Renou, Antonio Acín, and Matty J. Hoban (2023), “Quantum networks self-test all entangled states,” *Nature Physics* **19** (5), 670–675.
- Tura, J, R. Augusiak, A. B. Sainz, T. Vértesi, M. Lewenstein, and A. Acín (2014), “Detecting nonlocality in many-body quantum states,” *Science* **344** (6189), 1256–1258.
- Tura, J, R. Augusiak, A.B. Sainz, B. Lücke, C. Klempt, M. Lewenstein, and A. Acín (2015), “Nonlocality in many-body quantum systems detected with two-body correlators,” *Annals of Physics* **362**, 370–423.
- Vanderstraeten, Laurens, Jutho Haegeman, and Frank Verstraete (2019), “Tangent-space methods for uniform matrix product states,” *SciPost Physics Lecture Notes* , 7.
- Wang, Zizhu, and Damian Markham (2012), “Nonlocality of Symmetric States,” *Phys. Rev. Lett.* **108**, 210407.
- Yang, Kaiyan, Xiao Zeng, Yujing Luo, Guowu Yang, Lan Shu, Miguel Navascués, and Zizhu Wang (2022), “Contextuality in infinite one-dimensional translation-invariant local Hamiltonians,” *npj Quantum Information* **8** (1), 89.
- Zauner-Stauber, V, L. Vanderstraeten, M. T. Fishman, F. Verstraete, and J. Haegeman (2018), “Variational optimization algorithms for uniform matrix product states,” *Physical Review B* **97**, 045145.
- Zhang, Hao-Kai, Shuo Liu, and Shi-Xin Zhang (2024), “Absence of barren plateaus in finite local-depth circuits with long-range entanglement,” *Phys. Rev. Lett.* **132**, 150603.